PHYSICAL REVIEW E **81**, 065201(R) (2010)

Chimera states as chaotic spatiotemporal patterns

Oleh E. Omel'chenko,[1,2] Matthias Wolfrum,[1] and Yuri L. Maistrenko[2,3]
[1]*Weierstrass Institute for Applied Analysis and Stochastics, Mohrenstr. 39, 10117 Berlin, Germany*
[2]*Institute of Mathematics, National Academy of Sciences of Ukraine, Tereshchenkivska Str. 3, 01601 Kyiv, Ukraine*
[3]*National Center for Medical and Biotechnical Research, National Academy of Sciences of Ukraine, Volodymyrska Str. 54, 01030 Kyiv, Ukraine*

(Received 17 December 2009; revised manuscript received 18 May 2010; published 25 June 2010)

Chimera states are a recently new discovered dynamical phenomenon that appears in arrays of nonlocally coupled oscillators and displays a spatial pattern of coherent and incoherent regions. We report here an additional feature of this dynamical regime: an irregular motion of the position of the coherent and incoherent regions, i.e., we reveal the nature of the chimera as a spatiotemporal pattern with a regular macroscopic pattern in space, and an irregular motion in time. This motion is a finite-size effect that is not observed in the thermodynamic limit. We show that on a large time scale, it can be described as a Brownian motion. We provide a detailed study of its dependence on the number of oscillators N and the parameters of the system.

DOI: 10.1103/PhysRevE.81.065201 PACS number(s): 05.45.Xt, 89.75.Kd

I. INTRODUCTION

The so-called chimera states, discovered in 2002 by Kuramoto and Battogtokh [1], have recently attracted considerable attention [2–10]. Displaying a self-organized spatially intermittent pattern of regions with coherent and incoherent motion, they constitute a new paradigm of dynamical behavior that can serve as a prototype for various physical phenomena, e.g., coexistence of synchronous and asynchronous neural activity (so-called "bump" states) [11–14] or turbulent-laminar flow patterns [15]. From the point of view of synchronization theory [16–19] they can be considered as a remarkable example of partial frequency synchronization, appearing in a system of identical oscillators, where phase-locking occurs only in the coherent region. The most simple system that shows this type of behavior are arrays of coupled phase oscillators [20,21] that will be also used in this Rapid Communication. As in the Kuramoto-Sakaguchi system, a phase lag parameter has to induce a certain amount of repelling between the oscillators. Similarly, this could be provided also by a coupling delay [5,6]. From the point of view of classical pattern formation in spatially extended systems, the appearance of chimera states requires two essential ingredients: nonlocal coupling [3] and the discrete nature of the medium. Besides numerical experiments, a refined version of Kuramoto's self-consistency approach [8,10,22,23] for the thermodynamic limit up to now has been the main tool for their investigation.

In this Rapid Communication we focus our attention on the finite dimensional nature of the chimera states. We report an essential feature of the chimera state that is not captured by the self-consistency approach for the thermodynamic limit: whereas in earlier papers the chimera states have been described as a regime with time independent regions of coherent and incoherent motion, we point out that, on top of the chaotic motion within the incoherent region, *the coherent and incoherent region themselves show a chaotic motion* of their position on the unit circle. It turns out that, on a sufficiently large time scale, the motion of the chimera's position manifests itself as a Brownian motion. The main purpose of this Rapid Communication is to determine the properties of this motion, their scaling behavior with the number of oscillators, and their dependence on the system parameters as well as on the type of the coupling function.

II. MODEL

Our model is a ring of N identical nonlocally coupled phase oscillators with phases $\vec{\Psi}=(\Psi_1,\ldots,\Psi_N)$

$$\dot{\Psi}_k(t)=\omega-\frac{2}{N}\sum_{j=1}^{N}G(x_k-x_j)\sin(\Psi_k(t)-\Psi_j(t)+\alpha). \quad (1)$$

Here ω denotes the natural frequency of the oscillators that can be set to zero, and $\alpha\in(0,\pi/2)$ is a phase lag. The oscillators are assumed to be uniformly distributed over the interval $[-1,1]$ with positions $x_k=-1+2k/N$, $k=1,\ldots,N$. With these positions the coupling function $G(x)$ determines a nonlocal coupling on a macroscopic scale that is independent on the actual number of oscillators. We suppose that $G(x)$ is a nonnegative even function, which has to be 2-periodic to account for the ring topology of the network and is normalized to $\int_{-1}^{1}G(x)dx=1$. The simplest way to represent a nonlocal coupling is the steplike function

$$G_{step}(x,r)=\begin{cases}1/(2r), & \text{if } |x|\le r\\ 0, & \text{if } |x|>r\end{cases} \quad (2)$$

that has already been used in [24] for different purposes. Alternatively, one can use a cosine coupling function [3]

$$G_{\cos}(x,r)=\frac{1}{2}[1+r\cos(\pi x)] \quad (3)$$

or an exponentially decaying function [1].

III. SYMMETRIC AND ASYMMETRIC CHIMERA STATES

Chimera states are remarkable by the fact that they show in a homogeneous system the emergence of a spontaneous pattern, consisting of a coherent and an incoherent region.

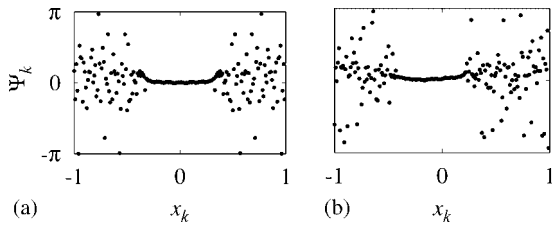

FIG. 1. Phase snapshots of (a) symmetric and (b) nonsymmetric chimera states. $N=200$.

According to [3,4], the main ingredients for their appearance in a system of form (1) are a Sakaguchi parameter α smaller, but close to $\frac{\pi}{2}$, and a nonlocal coupling. In contrast to earlier results, we present here also chimera states for a simple steplike coupling function. Figure 1 shows a typical fixed time snapshot of phases Ψ_k for a chimera state. In one part of the domain the oscillators are phase locked, whereas in the other part we observe an incoherent motion. Moreover, the time averages of the local phase velocities differ between the coherent and incoherent region. The average phase velocity profile can be determined by a Kuramoto-type self-consistency approach [1], see also Fig. 3(a).

As stated in [1,3], the initial data have to be carefully prepared, since the chimera state typically coexists with a stable coherent state. Figure 1(a) shows a chimera state with a reflection symmetry $\Psi_k=\Psi_{N-k+1}$ as presented in [3,4]. However, we were unable to reproduce this as a stable state of system (1). Instead, Fig. 1(a) has been obtained by artificially imposing this symmetry. Using a nonsymmetric scheme, we observed instability with respect to asymmetric perturbations, i.e., already arbitrarily small deviations from a symmetric state lead after a short period of integration to an asymmetric configuration, see Fig. 1(b). Moreover, in contrast to the chimera states with artificial symmetry, the asymmetric chimera states exhibit a further interesting behavior. Instead of being localized stationary patterns as reported earlier, they exhibit chaotic fluctuations of their position along the unit circle. It turns out that the itineracy of the chimera position depends sensitive on the initial condition. Figure 2 shows the motion of two chimera trajectories with initial conditions that differ only by 10^{-3}. We are now going to investigate in detail the stochastic properties of this irregular motion. To this end we have performed extensive simulations, using a Runge-Kutta scheme for numerical integration of system (1). As default parameters we used $\alpha=1.46$, $\omega=0$, and $r=0.7$ for the piecewise constant coupling function $G_{step}(x,r)$.

IV. DETERMINING THE POSITION OF A CHIMERA STATE

In order to analyze the motion of the chimera's position, we first have to find a way how to determine its instantaneous position. We decided for this purpose to make use of the spatial variation in the phase velocities. Following Kuramoto's self-consistency approach, one can determine a inhomogeneous profile of effective frequencies. This indicates that in average, the phase velocities in the incoherent domain

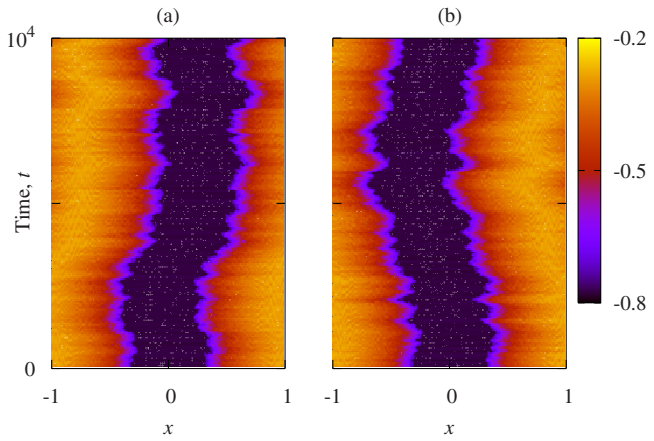

FIG. 2. (Color online) Sensitivity to initial conditions: two chimera trajectories with initial conditions that differ by 10^{-3}. (Color coded time-averaged phase velocities, dark region: coherent motion). $N=200$.

are faster than in the coherent domain and closer to the natural frequency of the oscillators that we have chosen here to be zero. Hence, for any fixed time moment, we compare the instantaneous phase velocities $\dot{\Psi}_k$ with a periodic reference profile $f(x,\xi)=-1-\cos\pi(x-\xi)$ and determine the position of a chimera at time t_0, given by $\tilde{\Psi}(t_0)$ as the value ξ, where the function

$$F(\xi) := \frac{1}{N}\sum_{k=1}^{N}[\dot{\Psi}_k(t_0) - f(x_k,\xi)]^2 \tag{4}$$

attains its global minimum. Figure 3 shows a time snapshot of phase velocities, their time average that can be determined from the self-consistency approach and the corresponding target function $F(\xi)$ from which we determine the position. In this way, we obtain for a chimera trajectory $\tilde{\Psi}(t)$ a time-dependent position $\xi(t)$ as given in Fig. 4. Note that on a small time scale it appears as a smooth function with irregular oscillations, whereas on larger time scales it shows properties of a stochastic motion.

V. STOCHASTIC PROPERTIES OF THE DETERMINISTIC MOTION OF THE POSITION

To reveal the nature of the chimera's motion, we present now the results of a stochastic analysis for the numerical

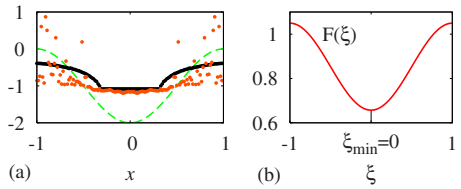

FIG. 3. (Color online) (a) Snapshot of phase velocities (orange/gray dots); time averaged phase velocities (black dots) following the profile given by Kuramoto's self-consistency equation. For the given phase velocities, the reference function $f(x,\xi)$ with $\xi=0$ (dashed green curve) minimizes the distance function $F(\xi)$ shown in (b).

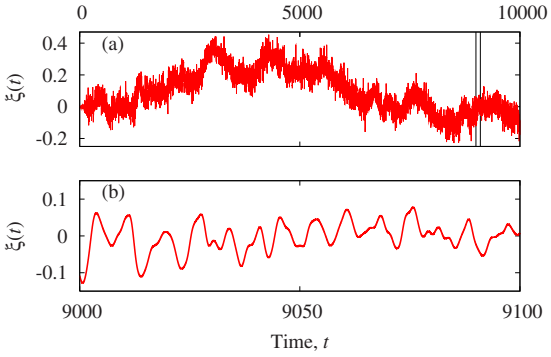

FIG. 4. (Color online) Time evolution $\xi(t)$ of a chimera's position, $N=200$: (a) Brownian motion on large time scales and (b) deterministic irregular oscillations on a short time scale.

simulation data obtained as described above. We start with the normalized autocorrelation function for the displacements

$$C(\tau) = \frac{\langle \dot{\xi}(t)\dot{\xi}(t+\tau)\rangle}{\langle \dot{\xi}^2(t)\rangle}, \tag{5}$$

and the characteristic correlation time

$$\tau_c = \int_0^\infty C^2(t)dt. \tag{6}$$

Figure 5 shows that the amplitude of $C(\tau)$ exponentially decays to zero. Moreover, it turns out that the correlation time τ_c does not significantly depend on N or on the other parameters. Based on this observation, we can treat the chimera's motion on sufficiently large time scales as a stationary stochastic process. Taking a sufficiently large time step Δt, we construct now from our simulation data a histogram of the increments $\Delta\xi$ of ξ in each time step. In order to eliminate the fast deterministic oscillations, we have used for this purpose local time averages of $\xi(t)$. Figure 6(a) shows that for fixed Δt their distribution can be nicely described by a Gaussian

$$\rho(\Delta\xi) = \frac{1}{\sqrt{2\pi\sigma(\Delta t)}} e^{-\Delta\xi^2/2\sigma(\Delta t)}, \tag{7}$$

with center at zero, and variance $\sigma(\Delta t)$. Extracting the variance $\sigma(\Delta t)$ for different values of Δt by a fitting procedure,

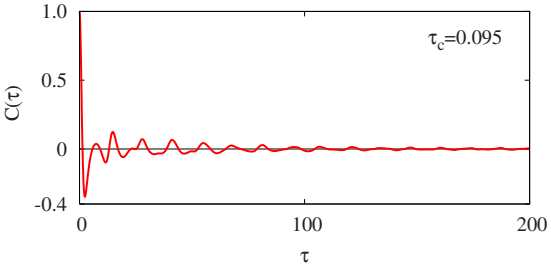

FIG. 5. (Color online) Normalized autocorrelation function (5) for $\xi(t)$ evaluated from a time interval $T=10^6$. $N=200$.

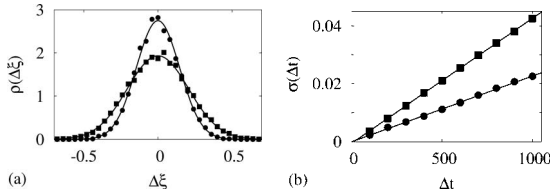

FIG. 6. (a) Histograms of displacements $\Delta\xi$ corresponding to $\Delta t=200$ (circles) and $\Delta t=600$ (squares) with fitted normal distribution [Eq. (7)] (solid lines). (b) Variance σ for coupling function $G_{step}(x,0.7)$ (squares) and $G_{\cos}(x,0.99)$ (circles) shows linear dependence on time step Δt [see Eq. (8)]. $N=100$.

we can represent the dependence $\sigma(\Delta t)$. Figure 6(b) shows that $\sigma(\Delta t)$ follows a linear dependence

$$\sigma(\Delta t) = 2D\Delta t \tag{8}$$

that can be used to extract the diffusion coefficient D of a corresponding Fokker-Planck equation. Hence, the chimera's motion can be described as a Brownian motion. In order to study the scaling behavior of the diffusion coefficient $D(N)$ with the number of oscillators N, we have repeated this procedure for values N varying from 60 to 800. Plotting the results in a double logarithmic scale, see Fig. 7, we obtain an almost perfect linear behavior with a slope of approximately -1.69, provided by a least-squares fitting. This number is surprisingly close to $-5/3$, however, we cannot provide at the moment a theoretical explanation why the diffusion coefficient should follow the power law $N^{-5/3}$. In any case, this observation underlines that the chimera's motion is a finite-size effect that vanishes in the thermodynamic limit, where the chimera state is neutrally stable with respect to shifts of its position. The growing instability for smaller N corresponds with the fact that for sufficiently small N ($N\approx 50$) it becomes difficult to observe the chimera regime at all. Instead, chimeralike states exist only as transients and collapse to a completely coherent state after a finite time.

VI. DEPENDENCE OF THE CHIMERA'S MOTION ON THE SYSTEM PARAMETERS

We present now some results on the dependence of the diffusion coefficient D on the phase lag parameter α and on the coupling radius r. Figure 8 shows the variation of D for different values of α and r. One can observe a clear dependence that is mainly correlated with the size of the coherent

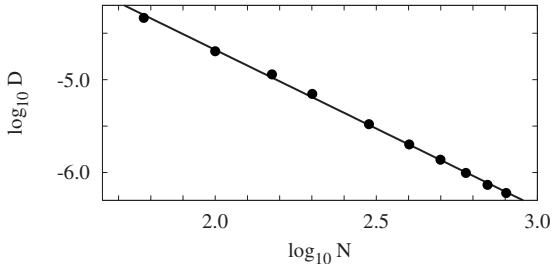

FIG. 7. The dependence of the diffusion coefficient D on the number of oscillators N follows a power law $D(N)\sim N^{-5/3}$.

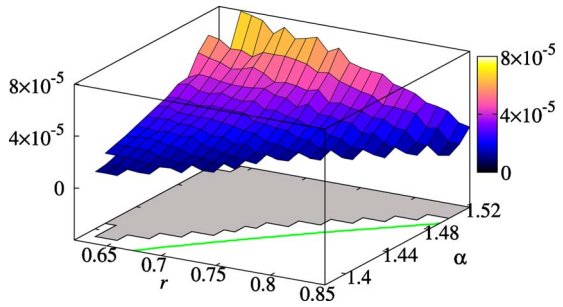

FIG. 8. (Color online) Dependence of the diffusion coefficient D on the coupling range r and the phase lag α. The gray region at the bottom indicates the parameter region, where we found chimera trajectories for $N=100$. The green (light gray) line indicates the boundary of the existence region for the limit $N=\infty$.

part. Indeed for chimera states with α close to $\frac{\pi}{2}$, where the coherent region is small [3,4], we obtain a large diffusion D. Also the type of coupling function has a significant impact on the size of the diffusion coefficient. Indeed, the motion is most pronounced for the steplike coupling function, where at the same number of oscillators, the diffusion coefficient D is typically by a factor of two bigger than for the cosine coupling function, see Fig. 6(b).

VII. CONCLUSIONS

In this Rapid Communication, we have investigated the spatiotemporal behavior of chimera states in arrays of nonlocally coupled phase oscillators. We show that chimera states exist also for steplike coupling functions. In contrast to [3,4], we were unable to find stable symmetric chimera states using an asymmetric scheme. For chimera states without artificially imposed symmetry, we observe a chaotic motion of the chimera's position along the unit circle. The motion shows a sensitive dependence on the initial data and is a finite-size effect that vanishes in the thermodynamic limit. We show that it can be described as a Brownian motion and study its dependence on the coupling coupling radius r, the phase lag parameter α, and the shape of the coupling function. For the corresponding diffusion coefficient D, we discovered for increasing number of oscillators N a scaling behavior $D(N)\sim N^{-5/3}$. This is rather uncommon for thermodynamic limits and resembles the famous Kolmogorov law for the energy distribution in turbulent flows [25].

ACKNOWLEDGMENT

We thank M. Hasler, A. Pikovsky, and A. Weiss for fruitful discussions.

[1] Y. Kuramoto and D. Battogtokh, Nonlinear Phenom. Complex Syst. (Minsk, Belarus) **5**, 380 (2002).
[2] S. I. Shima and Y. Kuramoto, Phys. Rev. E **69**, 036213 (2004).
[3] D. M. Abrams and S. H. Strogatz, Phys. Rev. Lett. **93**, 174102 (2004).
[4] D. M. Abrams and S. H. Strogatz, Int. J. Bifurcation Chaos Appl. Sci. Eng. **16**, 21 (2006).
[5] O. E. Omel'chenko, Y. L. Maistrenko, and P. A. Tass, Phys. Rev. Lett. **100**, 044105 (2008).
[6] G. C. Sethia, A. Sen, and F. M. Atay, Phys. Rev. Lett. **100**, 144102 (2008).
[7] D. M. Abrams, R. Mirollo, S. H. Strogatz, and D. A. Wiley, Phys. Rev. Lett. **101**, 084103 (2008).
[8] A. Pikovsky and M. Rosenblum, Phys. Rev. Lett. **101**, 264103 (2008).
[9] C. R. Laing, Chaos **19**, 013113 (2009).
[10] C. R. Laing, Physica D **238**, 1569 (2009).
[11] A. Compte, N. Brunel, P. S. Goldman-Rakic, and X.-J. Wang, Cereb. Cortex **10**, 910 (2000).
[12] A. Renart, P. Song, and X.-J. Wang, Neuron **38**, 473 (2003).
[13] C. C. Chow and S. Coombes, SIAM J. Appl. Dyn. Syst. **5**, 552 (2006).
[14] H. Sakaguchi, Phys. Rev. E **73**, 031907 (2006).
[15] D. Barkley and L. S. Tuckerman, Phys. Rev. Lett. **94**, 014502 (2005).
[16] A. Pikovsky, M. Rosenblum, and J. Kurths, *Synchronization: A Universal Concept in Nonlinear Sciences* (Cambridge University Press, Cambridge, 2001).
[17] A. Winfree, *The Geometry of Biological Time* (Springer, Berlin, 2001).
[18] S. Boccaletti, *Synchronized Dynamics of Complex Systems* (Elsevier, New York, 2008).
[19] E. Mosekilde, Y. Maistrenko, and D. Postnov, *Chaotic Synchronization: Application to Living Systems* (World Scientific, Singapore, 2002).
[20] Y. Kuramoto, *Chemical Oscillations, Waves, and Turbulence* (Springer, Berlin, 1984).
[21] S. H. Strogatz, Physica D **143**, 1 (2000).
[22] E. Ott and T. M. Antonsen, Chaos **18**, 037113 (2008).
[23] E. A. Martens, E. Barreto, S. H. Strogatz, E. Ott, P. So, and T. M. Antonsen, Phys. Rev. E **79**, 026204 (2009).
[24] D. A. Wiley, S. H. Strogatz, and M. Girvan, Chaos **16**, 015103 (2006).
[25] A. N. Kolmogorov, Dokl. Akad. Nauk SSSR **30**, 301 (1941).